online data

# Enzymes or redox couples? The kinetics of thioredoxin and glutaredoxin reactions in a systems biology context

Ché S. PILLAY, Jan-Hendrik S. HOFMEYR, Brett G. OLIVIER, Jacky L. SNOEP and Johann M. ROHWER[1]

Triple-J Group for Molecular Cell Physiology, Department of Biochemistry, Stellenbosch University, ZA-7602 Matieland, Stellenbosch, South Africa

Systems biology approaches, such as kinetic modelling, could provide valuable insights into how thioredoxins, glutaredoxins and peroxiredoxins (here collectively called redoxins), and the systems that reduce these molecules are regulated. However, it is not clear whether redoxins should be described as redox couples (with redox potentials) or as enzymes (with Michaelis–Menten parameters) in such approaches. We show that in complete redoxin systems, redoxin substrate saturation and other purported enzymatic behaviours result from limitations in the redoxin redox cycles in these systems. Michaelis–Menten parameters are therefore inappropriate descriptors of redoxin activity; data from redoxin kinetic experiments should rather be interpreted in terms of the complete system of reactions under study. These findings were confirmed by fitting kinetic models of the thioredoxin and glutaredoxin systems to *in vitro* datasets. This systems approach clarifies the inconsistencies with the descriptions of redoxins and emphasizes the roles of redoxin systems in redox regulation.

Key words: glutathione, kinetic modelling, NADPH, redoxin, reductase, thiol.

## INTRODUCTION

Thioredoxins, glutaredoxins and peroxiredoxins (which we collectively refer to as redoxins) are components of systems that are involved in a number of key redox reactions *in vivo* [1–7]. The thioredoxin system consists of thioredoxin and thioredoxin reductase, and the glutaredoxin system consists of glutaredoxin, glutathione and glutathione reductase (Figure 1). In these systems, reducing equivalents are transferred from NADPH to oxidized substrates via one or more coupled redox cycles. The roles of these systems in redox regulation are now being considered in a systems biology context [8].

A first step in any systems biology approach, such as kinetic modelling, is to define clearly the components under study. In the case of the redoxins, it is not immediately apparent whether they should be modelled as redox couples or as enzymes. Redox potentials and ratios of oxidized to reduced redoxin have been used to describe redoxins *in vivo* and *in vitro* [2,9–11], suggesting that redoxins should be modelled as redox couples. This approach has been adopted for modelling thioredoxins in a number of quantitative descriptions of the cellular redox environment [12–14].

On the other hand, in assays involving complete redoxin systems (Figure 1), redoxins have been quantified with Michaelis–Menten kinetic parameters [15–18], suggesting that they should be modelled as enzymes. Indeed, evidence has been presented that redoxins are Ping Pong enzymes (see for example [18–20]). There are, however, a number of inconsistencies in the description of redoxins as enzymes. For example, in contrast with the catalytic cycles of conventional enzymes, thioredoxins become inactive (oxidized) after reacting with their substrates (Figure 1). A separate enzyme-catalysed reaction is required to return thioredoxin to its active form. Other inconsistencies include a varying turnover number for the reduction of insulin by thioredoxin (compare with Table 1 in [15]), glutaredoxin substrates that do not have 'true' $K_M$ values [20], Michaelis–Menten parameters that underestimate the activity of yeast peroxiredoxins [21] and peroxiredoxins that do not show substrate saturation behaviour (see for example [22]).

Thus, any systems biology analysis of these redoxin systems is complicated firstly by the description of the redoxins themselves, and secondly by the inconsistencies with the description of redoxins as enzymes. We tested the possibility that these two problems are actually the same problem, namely that the enzymatic behaviours attributed to redoxins are mediated by the coupling of reactions in these redoxin systems. By analysing the complete set of reactions in these redoxin systems, we are able to provide a rational explanation for the inconsistencies with descriptions of redoxins and their reactions, and provide a framework for further analyses of these systems.

## EXPERIMENTAL

### Kinetic modelling

All kinetic modelling experiments were carried out using the open source PySCeS (Python Simulator for Cellular Systems) modelling software [23] (http://pysces.sourceforge.net). Two types of model were built: core models parameterized with arbitrary parameter sets that were used to investigate the generic kinetic behaviour of particular pathway structures, and detailed models parameterized with realistic parameter sets that were used to analyse the thioredoxin and glutaredoxin systems. Realistic parameter sets were obtained from primary literature sources, some of which were found using the BRENDA kinetic parameter database (http://www.brenda-enzymes.info). Kinetic models of the thioredoxin and glutaredoxin systems were fitted to *in vitro* datasets using non-linear least squares regression with the Levenberg–Marquardt algorithm, available through the SciPy library of scientific routines (http://www.scipy.org). All models have been made available on the JWS Online database [24]. In addition, all model parameters are available in the Supplementary

Abbreviations used: Grx1, glutaredoxin 1; Grx(SH)$_2$, reduced glutaredoxin; Grx(SS), oxidized glutaredoxin; PSSG, SQLWC(glutathione)LSN; Trx(SH)$_2$, reduced thioredoxin; Trx(SS), oxidized thioredoxin.

[1] To whom correspondence should be addressed (email jr@sun.ac.za).

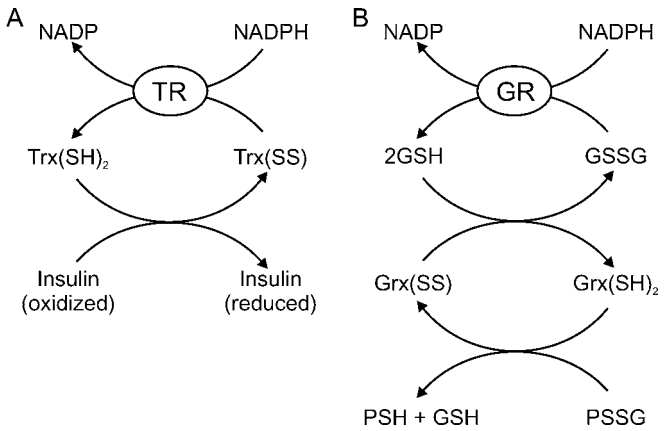


**Figure 1 A comparison of the reaction schemes for the thioredoxin and glutaredoxin systems**

In the thioredoxin insulin assay system (**A**), reduced thioredoxin [$Trx(SH)_2$] reduces oxidized insulin and is consequently oxidized [Trx(SS)]. Oxidized thioredoxin is in turn reduced by thioredoxin reductase (TR) with NADPH as a source of reducing equivalents [15,19,31]. In a glutaredoxin system (**B**), a glutathionylated peptide (PSSG) is reduced by $Grx(SH)_2$, which is in turn reduced by glutathione (GSH). Oxidized glutathione (GSSG) is reduced by glutathione reductase (GR) with NADPH as a source of reducing equivalents.

Data provided with this paper, at http://www.BiochemJ.org/bj/417/bj4170269add.htm.

## RESULTS

### An analytical solution of a single-cycle redoxin system

The redox cycling of redoxins (Figure 1) is a common motif found in all redoxin systems. A generic model of a single cycle redoxin system (Scheme 1) was analysed to determine what influence this cycling has on the kinetics of the redoxin oxidation-substrate reduction reaction in this system.

Scheme 1

$$A + M \leftrightarrow B + M' \quad (1)$$

$$C + M' \leftrightarrow D + M \quad (2)$$

In this analysis, capitalized letters represent species names, whereas lower-case letters represent concentrations. The scheme consists of two reactions, (1) and (2), linked by redoxin molecules, $M$ and $M'$, representing the oxidized and reduced forms of a given redoxin (compare with thioredoxin, Figure 1). Reaction (1) represents the oxidation of $A$ to $B$ with the concomitant reduction of $M$ to $M'$, whilst reaction (2) represents the reduction of $C$ to $D$ with the concomitant oxidation of $M'$ to $M$. The $M$ and $M'$ redoxin molecules constitute a moiety conserved couple [25,26] with the constant sum of their concentrations described by $m_t$.

To simplify the analysis, reactions (1) and (2) were assumed to obey reversible mass-action kinetics and were described by rates $v_1$ and $v_2$ with respective forward rate constants $k_1$ and $k_2$, and reverse rate constants $k_{-1}$ and $k_{-2}$. Reaction (1) would be catalysed by thioredoxin reductase in the thioredoxin system (Figure 1). Therefore, $k_1$ actually represents an aggregate of a number of other parameters, including the thioredoxin reductase concentration in this system. Substrate reduction by thioredoxins and glutaredoxins (compare with reaction 2) proceeds via the formation of a mixed disulfide complex between the redoxin and its respective substrate (see for example [27,28]). For thioredoxin reactions, the formation of this complex may proceed via two kinetically distinct routes [29]. Once formed, the breakdown of these redoxin–substrate complexes is highly favourable and the complexes are not significantly populated under normal conditions (see for example [9,16,28]). On the basis of this, the intermediate steps involving the mixed disulfide complex were not explicitly modelled, and were instead aggregated into a single mass-action kinetic expression for the entire reaction (reaction 2). The validity of this simplification was tested by fitting kinetic models of the thioredoxin and glutaredoxin systems to realistic data sets (see below).

In substrate saturation assays the concentration of the oxidized 'substrate' of the redoxin, in this case $C$ (Scheme 1), would be increased and $v_1$ or $v_2$ monitored. Typically, the reaction would appear to saturate as the concentration of the redoxin substrate was increased (see for example [15–18]).

Scheme 1 can be described with the following equations:

$$\frac{dm'}{dt} = k_1 am - k_{-1} bm' - k_2 cm' + k_{-2} dm \quad (3)$$

$$m' = m_t - m \quad (4)$$

$$v_2 = k_2 m'c - k_{-2} md \quad (5)$$

**Table 1 Changes in the parameters of a thioredoxin assay kinetic model affect the steady-state behaviour and apparent Michaelis–Menten kinetic parameters for the reduction of insulin by thioredoxin**

Kinetic parameters of a model of the thioredoxin system (Figure 1) were varied and the effect on the steady-state fluxes, redoxin concentrations and Michaelis–Menten kinetic parameters determined. The parameters that were varied were: the limiting rate for thioredoxin reductase ($V_{TR}$), the second-order rate constant for insulin reduction ($k_2$), the total thioredoxin concentration ($[Trx]_t$) and the NADPH concentration. The goodness of fit to the Lineweaver–Burk plot is given by an $r^2$ value. [$Trx(SH)_2$] and [Trx(SS)], concentration of $Trx(SH)_2$ and Trx(SS). All concentrations are in $\mu$M. $V_{max}$ and flux values are in $\mu M \cdot min^{-1}$, $k_{cat}$ values in $min^{-1}$, and $k_2$ and $k_{cat}/K_m$ values are in $\mu M^{-1} \cdot min^{-1}$.

| Model parameters | | | | Steady state results | | | Apparent Michaelis–Menten parameters | | | | |
|---|---|---|---|---|---|---|---|---|---|---|---|
| $V_{TR}$ | $k_2$ | $[Trx]_t$ | NADPH | [Trx(SS)] | $[Trx(SH)_2]$ | Flux | $K_m$ | $V_{max}$ | $k_{cat}$ | $k_{cat}/K_m$ | $r^2$ |
| 1 | 1 | 2 | 1 | 1.686 | 0.314 | 0.314 | 0.186 | 0.386 | 0.193 | 1.035 | 0.999 |
| 10 | 1 | 2 | 1 | 0.449 | 1.551 | 1.551 | 2.183 | 4.378 | 2.189 | 1.003 | 1.000 |
| 100 | 1 | 2 | 1 | 0.004 | 1.959 | 1.959 | 21.925 | 43.860 | 21.930 | 1.000 | 1.000 |
| 1 | 10 | 2 | 1 | 1.967 | 0.033 | 0.331 | 0.012 | 0.348 | 0.174 | 14.620 | 0.985 |
| 1 | 100 | 2 | 1 | 1.997 | 0.003 | 0.333 | 0.001 | 0.333 | 0.167 | 263.158 | 0.999 |
| 1 | 1 | 50 | 1 | 49.510 | 0.490 | 0.490 | 0.001 | 0.496 | 0.010 | 8.333 | 0.803 |
| 1 | 1 | 0.1 | 1 | 0.068 | 0.032 | 0.032 | 0.462 | 0.046 | 0.463 | 1.002 | 1.000 |
| 1 | 1 | 2 | 10 | 1.460 | 0.540 | 0.540 | 0.356 | 0.724 | 0.362 | 1.018 | 0.999 |
| 1 | 1 | 2 | 0.1 | 1.940 | 0.060 | 0.060 | 0.026 | 0.065 | 0.032 | 1.236 | 0.991 |

At steady state, eqn (3) is zero. Substituting eqn (4) into eqn (3) and solving for $m$ yields the following expression:

$$m = \frac{m_t(k_{-1}b + k_2c)}{k_1a + k_{-2}d + k_{-1}b + k_2c} \quad (6)$$

Substituting eqns (4) and (6) into eqn (5) yields:

$$v_2 = \frac{k_1k_2m_tac\left(1 - \frac{\Gamma}{K_{eq}}\right)}{k_1a + k_{-2}d + k_{-1}b + k_2c} \quad (7)$$

where $\Gamma$ is the mass-action ratio $[\Gamma = bd/(ac)]$ and $K_{eq} = k_1k_2/(k_{-1}k_{-2})$.

When reactions (1) and (2) are assumed to be irreversible, i.e. $k_{-1} = k_{-2} = 0$, eqn (7) simplifies to:

$$v_2 = \frac{(k_1am_t)c}{\frac{k_1}{k_2}a + c} \quad (8)$$

Eqn (8) has the same form as the Michaelis–Menten equation with an apparent $V_{max}$ described by $k_1am_t$, an apparent $k_{cat}$ described by $k_1a$, and an apparent $K_m$ described by $k_1a/k_2$. The ratio $k_{cat}/K_m$ is therefore equal to $k_2$. Thus reaction (2), which has mass-action kinetics will, when coupled to reaction (1), saturate with increasing concentrations of reactant $C$. In assays involving these redoxin systems, it has been assumed that substrate saturation behaviour reflected the saturation of the redoxins themselves and Michaelis–Menten kinetic parameters have consequently been assigned to these redoxins (see for example [15–18]). This analytical solution demonstrates that this saturation behaviour is an inherent property of these systems.

Eqn (8) also shows that the apparent $K_m$ and $V_{max}$ values assigned to these redoxins are not true kinetic parameters, as both the apparent $k_{cat}$ and $K_m$ in eqn (8) depend on the concentration of $A$ and on $k_1$. Thus, for example, in substrate saturation studies involving the thioredoxin system, the apparent $K_m$ and $k_{cat}$ would vary with the NADPH concentration and with the concentration of the thioredoxin reductase used in these assays. This provides an explanation for inconsistencies with the Michaelis–Menten parameters that have been assigned to these redoxins.

Glutaredoxins and peroxiredoxins are components of systems that have at least two moiety conserved cycles [3,6,30]. The analytical rate equations for such systems are extremely complex and will not be considered here.

### Thioredoxin insulin assay system

The Michaelis–Menten parameters for the reduction of insulin by thioredoxin were reported by Holmgren [15,19,31]. In keeping with the predictions from the analysis of eqn (8), the apparent $k_{cat}$ for the reduction of insulin by thioredoxin varied between 12–740 $min^{-1}$ with changes in proportions of the constituents of the assay (compare with Table 1 in [15]). This variation is inconsistent with an enzyme-catalysed reaction.

We therefore developed a kinetic model of the thioredoxin/insulin assay system (Figure 1A) using mass-action kinetics for the reduction of insulin by thioredoxin. The thioredoxin reductase reaction was described by a two-substrate Michaelis–Menten rate expression. Both reactions were described with irreversible expressions, which was consistent with the experimental conditions of the assay [15]. The second-order rate constant for the reduction of insulin by thioredoxin was determined by fitting the model to a dataset in the Holmgren paper (compare with Figure 2B in [15]).

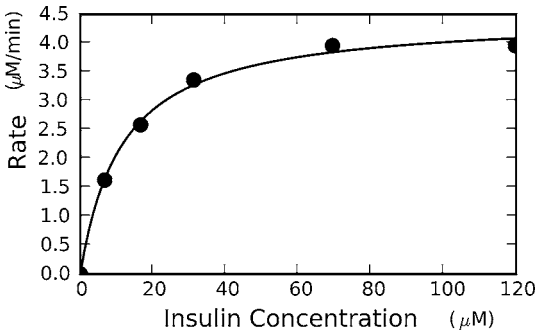


**Figure 2 A kinetic model of the thioredoxin/insulin assay showed an excellent fit to an *in vitro* dataset**

The kinetic model of Figure 1(A) was fitted to an *in vitro* dataset (●) reported by Holmgren (compare with Figure 2B in [15]). The kinetic model used mass-action kinetics for insulin reduction, and used a fitted second-order rate constant for insulin reduction by thioredoxin of $3.82 \pm 0.29\ \mu M^{-1} \cdot min^{-1}$ (see text for details). Quality of fit was excellent ($r^2 = 0.997$).

It was reported that the reduction of insulin by thioredoxin had an apparent $K_m$ of 11 $\mu$M and a $V_{max}$ of approximately $4\ \mu M \cdot min^{-1}$ [15]. An apparent $k_{cat}/K_m$ of $3.78\ \mu M^{-1} \cdot min^{-1}$ was obtained from these data. Using non-linear least squares regression, we determined a second-order rate constant for the reduction of insulin of $3.82 \pm 0.29\ \mu M^{-1} \cdot min^{-1}$. As predicted by eqn (8), this value was in agreement with the $k_{cat}/K_m$ determined from the original data. The kinetic model was an excellent fit of the *in vitro* dataset ($r^2 = 0.997$, Figure 2).

The model was parameterized with this fitted rate constant, and the initial oxidized insulin concentration was varied over the range of values reported in the original paper [15]. The resulting dataset was linearly transformed into a Lineweaver–Burk plot, and the apparent $K_m$ of thioredoxin with respect to insulin was determined as 12.12 $\mu$M. This value approximated to the apparent $K_m$ of 11 $\mu$M reported in the original paper [15].

### Substrate saturation in redoxin systems

Kinetic models of the thioredoxin system and a generic two-cycle redoxin system were then analysed to elucidate the mechanism behind substrate saturation in these systems. These models were parameterized with basic parameter sets (Table 1, parameters not shown for the two-cycle system) so that general kinetic behaviour in these systems could be investigated.

The generic two-cycle redoxin system model consisted of three reactions (Scheme 2):

Scheme 2

$$\text{NADPH} + M' \rightarrow \text{NADP}^+ + M' \quad (9)$$

$$M' + N \rightarrow M + N' \quad (10)$$

$$N' + C \rightarrow N + D \quad (11)$$

In this model, $N$ and $N'$ are the oxidized and reduced forms of a redoxin involved in the reduction of $C$ (reaction 11). This reaction was assigned mass-action kinetics. Compared with the thioredoxin system, the reduction of $N$ involves an additional redox reaction (reaction 10), which was also assigned mass-action kinetics. The concentration sums for the $N/N'$ and $M/M'$ redox couples were $n_t$ and $m_t$ respectively. The reductase reaction (reaction 9) was modelled with irreversible Michaelis–Menten kinetics.

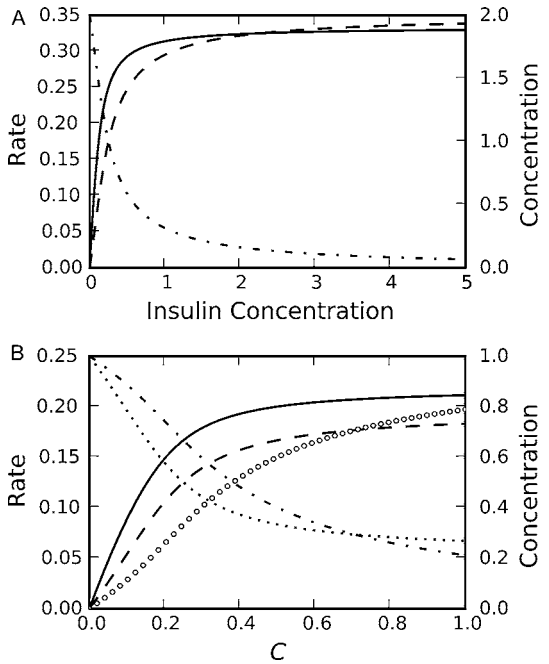


**Figure 3 Substrate saturation of redoxin systems is caused by limitations in redoxin reduction relative to redoxin oxidation**

(**A**) In a model of the thioredoxin system, the rate of insulin reduction (continuous line) appeared to saturate with increases in the insulin concentration. These increases resulted in limitations in oxidized thioredoxin reduction relative to $Trx(SH)_2$ oxidation, causing changes to concentrations of $Trx(SH)_2$ (dash-dot line) and Trx(SS) (broken line) (see text for details). (**B**) Similarly, a generic model of a two-cycle redoxin system (Scheme 2) also showed saturation with increases in the concentration of the redoxin substrate, *C* (continuous line). Increases in *C* resulted in the distribution of the reduced redoxin, *N*′ (dash-dot line), into its oxidized form *N* (○). A similar distribution was noted for the second redox couple in the system *M*′ (dotted line) and *M* (broken line).

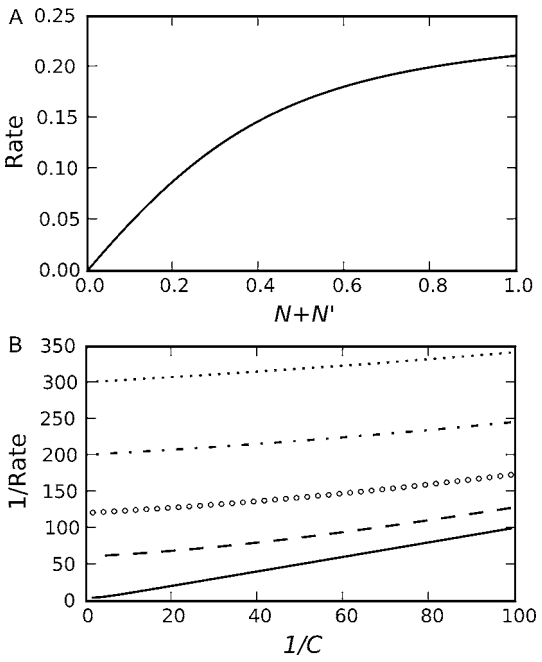


**Figure 4 The purported enzymatic behaviour of redoxins in two-cycle redoxin systems is an inherent property of these systems**

A generic kinetic model of a two-cycle redoxin system (Scheme 2) displayed a number of behaviours that were consistent with an enzymatic mechanism. In (**A**), as the total concentration of the redoxin, $N + N'$, was increased, the rate of *C* reduction appeared to increase linearly at low concentrations of redoxin. In (**B**), the kinetic model displayed apparent Ping Pong behaviour with respect to *M* and *C*. The concentrations of $M + M'$ for each simulation were 0.010 (dotted line), 0.015 (dash-dot line), 0.025 (○), 0.050 (broken line) and 1.000 (continuous line). These models were parameterized with basic kinetic parameter sets (see text).

In both models, increases in the redoxin oxidation reactions, owing to increased substrate concentrations, were accompanied by the conversion of the redoxin moieties into their oxidized forms (Figures 3A and 3B). These results showed that saturation occurred when increases in the redoxin substrate concentration could no longer lead to increases in the fluxes of the redoxin redox cycles in these systems. Thus the calculated $V_{max}$ values for the thioredoxin system were approximately equal to the maximal achievable rate of the thioredoxin reductase reactions in these simulations (Table 1, eqn 8).

## Michaelis–Menten parameters are inadequate descriptors of redoxin reactions

Apparent Michaelis–Menten parameters were determined for the thioredoxin and generic two-cycle kinetic models described above (Table 1, results not shown for the two-cycle system). Changes in values of some of the parameters in these models, such as the NADPH and reductase concentrations, resulted in changes to the apparent Michaelis–Menten parameters of these systems. These changes were consistent with the analytical solution of the system (eqn 8). For example, increases in the $V_{max}$ of the thioredoxin reductase resulted in increases in the apparent $K_m$ and $k_{cat}$ for insulin reduction (Table 1). From eqn (8), it would be expected that increases in the forward rate constant, $k_1$, would also result in corresponding increases in the apparent $K_m$ and $k_{cat}$ for insulin reduction.

As predicted by eqn (8), some of the $k_{cat}/K_m$ determinations from these simulations showed a good correlation with the second-order rate constants defined in the thioredoxin insulin assay model. However, even with these ideal datasets, some significant deviations were noted. For example, increases in $k_2$ resulted in significant differences between its value and the $k_{cat}/K_m$ determination from the simulations. In addition, high concentrations of thioredoxin resulted in biphasic plots (results not shown) whose apparent $k_{cat}/K_m$ also over-estimated the second-order rate constant for insulin reduction.

## Other kinetic behaviours of generic two-cycle redoxin systems

Apart from substrate saturation effects, assays of two-cycle redoxin systems have shown additional characteristics that appear consistent with enzymatic behaviour. For example, it has been reported that the rate of substrate reduction by these systems increases linearly with increases in redoxin concentration (see for example [16]). We tested whether our generic two-cycle kinetic model could account for this kinetic behaviour.

When the concentration of the redoxin in this model (i.e. $n_t$) was increased, there was a corresponding linear increase in the rates through the system at relatively low concentrations of redoxin (Figure 4A). This effect mimics the increases in rate that occur when the concentration of an enzyme is increased in a reaction. However, at higher concentrations of redoxin, the increase was no longer linear as the redox cycles in the system began to saturate (results not shown). This effect, which is inconsistent with an enzyme-catalysed reaction, has been reported in the literature. For a number of glutaredoxins, the rate of insulin reduction increased linearly with low concentrations of glutaredoxin, but saturated at higher concentrations (compare with Figure 7 in [32]).

It has also been reported that redoxins display Ping Pong kinetics with respect to their reducing and oxidizing 'substrates' in assays of these systems (see for example [18,20]). To determine whether the generic two-cycle model could display this behaviour, the concentrations of the redoxin 'substrates' ($M'$ and $C$) were both varied in the model, and the effect on the system flux was calculated. Linear transforms of these datasets showed apparent Ping Pong kinetics (Figure 4B), demonstrating that this behaviour is an inherent property of such systems. As $m_t$ was increased in these simulations, the resultant plots in Figure 4(B) appeared to group together owing to the saturation of the reductase reaction with increasing concentrations of $M$ (results not shown).

### Kinetic model of peptide deglutathionylation by Grx1 (glutaredoxin 1)

To illustrate the validity of a systems approach in describing realistic two-cycle redoxin systems, an *in vitro* dataset was fitted to a kinetic model of the deglutathionylation of a peptide substrate, PSSG [SQLWC(glutathione)LSN], by Grx1 (Figure 1, Scheme 3). In the original experiments of Peltoniemi et al. [16], the apparent Michaelis–Menten kinetic parameters for the reduction of this peptide by Grx1 were determined with substrate saturation experiments (compare with Figure 3B in [16]). In addition, the effects of increasing concentrations of Grx1 and GSH on rates were also reported [16].

Glutaredoxins can reduce substrates via monothiol and/or dithiol mechanisms [33,34]. Peltoniemi et al. [16] reported that Grx(SS) (oxidized Grx) was the only reaction intermediate that could be obtained in quenched and stopped-flow experiments involving Grx1 and PSSG, and it was reported that the rate of PSSG reduction by Grx1 showed a sigmoidal dependence on the GSH concentration. These results are consistent with a dithiol mechanism, and the model was accordingly described this way. The kinetic model of this system consisted of three reactions: the reduction of GSSG by glutathione reductase (reaction 12), the reduction of Grx(SS) by GSH (reaction 13) and the deglutathionylation of PSSG by Grx1 (reaction 14).

Scheme 3

$$\mathrm{NADPH} + \mathrm{GSSG} \rightarrow \mathrm{NADP} + 2\,\mathrm{GSH} \quad (12)$$

$$2\,\mathrm{GSH} + \mathrm{Grx(SS)} \rightarrow \mathrm{GSSG} + \mathrm{Grx(SH)_2} \quad (13)$$

$$\mathrm{Grx(SH)_2} + \mathrm{PSSG'} \rightarrow \mathrm{Grx(SS)} + \mathrm{PSH} + \mathrm{GSH} \quad (14)$$

Reaction (12) is essentially irreversible [35] and was modelled with the irreversible form of a generic two-substrate rate expression [36]. In keeping with the approach advocated in this paper, reactions (13–14) were modelled with mass-action kinetics. The equilibrium constant for reaction (13) was determined from the redox potentials of the glutaredoxin and glutathione redox couples as $1.37 \times 10^{-6}\ \mu\mathrm{M}^{-1}$ [9]. However, the equilibrium constant for reaction (14) was not known, and this reaction was therefore modelled with irreversible kinetics.

The rate constants for the glutaredoxin reduction and oxidation reactions were determined by fitting the kinetic model to an experimental dataset (Figure 3B in [16]) as described in the Experimental section. The kinetic model showed an excellent fit to this dataset ($r^2 = 0.990$, Figure 5A). The rate constant for the reduction of Grx1 by glutathione was determined as $4.78 \pm 0.34 \times 10^{-6}\ \mu\mathrm{M}^{-2} \cdot \mathrm{s}^{-1}$, whereas the rate constant for the reduction of the glutathionylated peptide by Grx1 was determined as $0.64 \pm 0.05\ \mu\mathrm{M}^{-1} \cdot \mathrm{s}^{-1}$. The latter rate constant again correlated with the apparent $k_{cat}/K_m$ of $0.56\ \mu\mathrm{M}^{-1} \cdot \mathrm{s}^{-1}$ reported for this system [16].

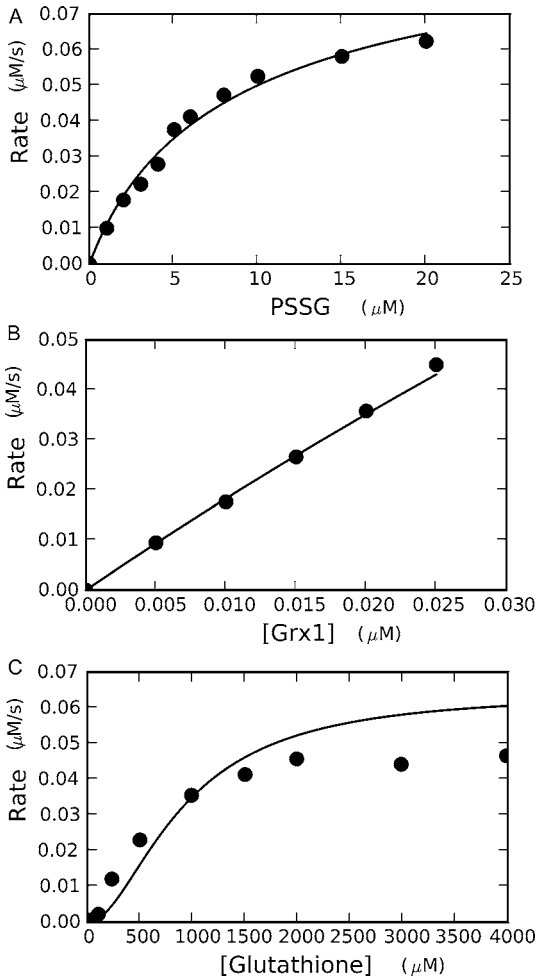


**Figure 5 A comparison between a kinetic model of the glutaredoxin-dependent deglutathionylation of a peptide, PSSG, by Grx1 (Scheme 3) and an *in vitro* dataset [16]**

In (**A**), the rate constants for the reduction of Grx1 and the deglutathionylation of PSSG were determined by fitting the kinetic model to an *in vitro* dataset reported by Peltoniemi et al. (●, compare with Figure 3B in [16]). Goodness of fit was assessed by an $r^2$ value of 0.990. The rate constant for the reduction of Grx1 by glutathione was determined to be $4.78 \pm 0.34 \times 10^{-6}\ \mu\mathrm{M}^{-2} \cdot \mathrm{s}^{-1}$, and the rate constant for the reduction of PSSG by Grx1 was determined to be $0.64 \pm 0.05\ \mu\mathrm{M}^{-1} \cdot \mathrm{s}^{-1}$. To validate these constants, kinetic models incorporating these rate constants were then compared with two independent *in vitro* datasets that had not been used in the fitting procedure. In (**B**), the effect of changing the concentration of Grx1 on rate was compared between the kinetic model (continuous line) and an *in vitro* dataset (●, compare with Figure 3A in [16]). In (**C**), the effect of changing the glutathione concentration on rate was compared between the kinetic model (continuous line) and an *in vitro* dataset (●, compare with Figure 3C in [16]).

To confirm whether the values obtained for the above rate constants were accurate, a kinetic model with these fitted parameters was then simulated to determine how well it corresponded to two independent datasets (compare with Figures 3A and 3C in [16]) that had not been used in the fitting procedure. The model results were in excellent agreement with an *in vitro* dataset that described the effect of increases in glutaredoxin concentration on the system rate (Figure 5B). The model also showed a good correlation with a dataset that described the effect of changes in glutathione concentration on rate (Figure 5C). In keeping with the GSH stoichiometry in reaction (13), the rate of NADPH oxidation in the kinetic model showed a sigmoidal dependence on the GSH

concentration in the system. The differences between the kinetic model and this experimental dataset were probably due to two reasons. Firstly, the kinetics of Grx1 reduction by GSH may require a more complex rate expression than the simple mass-action kinetic expression used here (reaction 13). The reduction of Grx1 by GSH proceeds via a Grx1–GSH mixed disulfide complex which is present at significant concentrations at equilibrium [9]. However, the concentration of this complex varies depending on the quenching procedure used in these experiments [9], which complicates the modelling of this reaction. Secondly, reaction (14) could only be modelled with irreversible kinetics. Thus, the effect of high GSH concentrations on the rate through this reaction would not be accounted for in this kinetic model.

## DISCUSSION

Systems approaches are now being explored so that an integrated view of redoxins in redox regulation and oxidative stress can be developed (see for example [14]). However, it is not clear whether redoxins should be modelled as redox couples or as enzymes in such approaches. For example, thioredoxins and glutaredoxins been described as Ping Pong enzymes [19,20]. It is difficult to reconcile this view, firstly, with the reaction schemes of thioredoxins (compare with Figure 1), and secondly, with studies that have found that the oxidized ('inactive') forms of these redoxins are present at significant concentrations *in vivo* [2,11,14,37]. Complicating this situation even further are a number of inconsistencies with the description of redoxin activity with Michaelis–Menten kinetic parameters (see the Introduction).

The roles played by the coupling of reactions in these redoxin systems in the purported enzymatic behaviour, and steady-state concentrations of these redoxins, have largely been neglected in the biochemical literature. We hypothesized that the apparently disparate descriptions of the redoxins could be reconciled by taking into account the kinetics of these redoxin systems as a whole.

As a first step, we considered the kinetics of a redoxin redox cycle, which is a basic motif in these systems. An analytical solution of this system (eqn 8) confirmed that the saturation of redoxin oxidation reactions is an inherent property of these cycles. This solution, together with the kinetic modelling results (Figures 3A and 3B), showed that substrate saturation of redoxin reactions is caused by limitations in the redoxin reduction relative to the redoxin oxidation reactions in these systems. In addition, a two-cycle kinetic model that used mass-action kinetics for redoxin oxidation and reduction displayed apparent Ping Pong kinetics (Figure 4B). Taken together, these results demonstrate that *in vitro* data from redoxin kinetic experiments should be interpreted in terms of the complete system of reactions under study. Similarly, data on the ratios of oxidized to reduced redoxin *in vivo* (see for example [2,11,14,37]) reflect the relative rates of redoxin oxidation to redoxin reduction in these systems (Table 1).

The analytical solution (eqn 8) and kinetic modelling results (Table 1) have also shown that the Michaelis–Menten kinetic parameters assigned to redoxins are sensitive to the concentrations of the other components in these redoxin systems. These results provide an explanation for the reported variation in the apparent $k_{cat}$ for insulin reduction by thioredoxin (compare with Table 1 in [15]), and for other inconsistencies that arise from the use of Michaelis–Menten parameters for quantifying redoxin activity. We therefore conclude that Michaelis–Menten kinetic parameters are inappropriate descriptors of redoxin activity.

Although Michaelis–Menten parameters are not valid descriptors of redoxin activity, analysis of eqn (8) showed that the second-order rate constants for redoxin oxidation reactions could be estimated from the $k_{cat}/K_m$ ratios reported for these redoxin systems. Indeed, the second-order rate constants determined from the fitting of our kinetic models to experimental datasets (Figures 2 and 5A) were in agreement with the $k_{cat}/K_m$ ratios reported in the original papers [15,16]. However, other modelling results have indicated that, depending on the system, these $k_{cat}/K_m$ estimates may vary significantly from the true second-order rate constants for these reactions (Table 1). Ogusucu et al. [21] directly determined second-order rate constants for a number of yeast peroxiredoxins. These rate constants were significantly higher than the $k_{cat}/K_m$ estimations from a previous study [38]. An initial kinetic modelling analysis of this peroxiredoxin system has established this effect (C.S.P., unpublished work).

To confirm the analytical solution and the generic modelling results described above, *in vitro* datasets were fitted to realistic kinetic models of the thioredoxin and glutaredoxin systems (Figures 2 and 5A). Both models showed excellent fits to their respective experimental datasets ($r^2 \geqslant 0.99$), suggesting that the models were consistent with the *in vitro* data. Moreover, when the fitted rate constants from the glutaredoxin system were used to parameterize a glutaredoxin kinetic model, the modelling results correlated well with two independent *in vitro* datasets that had not been used in the fitting procedure (Figures 5B and 5C). Collectively, these results provided convincing evidence that mass-action kinetics were sufficient to describe the redoxin oxidation reactions in these systems, and that consistent parameter sets could be obtained by fitting kinetic data to the complete redoxin system under study.

In systems biology, the construction of kinetic models is becoming increasingly important in order to understand and quantify how complex systems such as pathways within the living cell are regulated. The approach advocated by our group and others is to integrate kinetic data on the individual parts of the system (typically obtained from *in vitro* experiments on the isolated components) into such models, and then to see if these models can reproduce the *in vivo* behaviour of the intact system. This has been termed the 'silicon cell approach' [39]. In this context, it is crucial that existing *in vitro* data be correctly interpreted, and our work shows that mass-action rather than Michaelis–Menten kinetics are appropriate descriptors of redoxin activity.

The work presented here has reconciled the apparently disparate descriptions of the redoxins into a consistent quantitative framework. The enzymatic properties and the non-enzymatic reaction scheme for thioredoxin reduction/oxidation, the *in vivo* redox ratios of redoxins, and the reported inconsistencies that have arisen from the use of Michaelis–Menten parameters for quantifying redoxin activity can all be rationally explained in terms of this framework, which differs significantly from current models of redoxin systems. For example, in some models, the thioredoxin system has been equated to an electrical circuit with thioredoxin being a 'central node' or 'rheostat' that distributes reducing equivalents from thioredoxin reductase and NADPH to a number of independent processes [8,14,40]. In the framework proposed here, the thioredoxin redox cycle is central to redox regulation and signalling. This cycle would not only impose fixed limits on the fluxes through thioredoxin-dependent processes (Figure 3), but would also couple these processes to each other by virtue of their effects on the redox cycle. Just as the theoretical framework for ultrasensitivity in signal transduction pathways [41,42] led to the subsequent large-scale experimental analysis of this phenomenon (see for example [43]), it is hoped that the redoxin framework presented here will encourage the adoption of systems biology approaches in the study of redoxins and their systems.

C. S. P. is a recipient of a National Research Foundation (South Africa) Innovation Post-Doctoral Fellowship and B. G. O. is a recipient of a National Bioinformatics Network (South Africa) Post-Doctoral Fellowship.

## REFERENCES


1 Arner, E. S. and Holmgren, A. (2000) Physiological functions of thioredoxin and thioredoxin reductase. Eur. J. Biochem. **267**, 6102–6109
2 Watson, W. H., Yang, X., Choi, Y. E., Jones, D. P. and Kehrer, J. P. (2004) Thioredoxin and its role in toxicology. Toxicol. Sci. **78**, 3–14
3 Fernandes, A. P. and Holmgren, A. (2004) Glutaredoxins: glutathione-dependent redox enzymes with functions far beyond a simple thioredoxin backup system. Antioxid. Redox Signal. **6**, 63–74
4 Vlamis-Gardikas, A. and Holmgren, A. (2002) Thioredoxin and glutaredoxin isoforms. Methods Enzymol. **347**, 286–296
5 Halliwell, B. (2006) Reactive species and antioxidants. Redox biology is a fundamental theme of aerobic life. Plant Physiol. **141**, 312–322
6 Rhee, S. G., Chae, H. Z. and Kim, K. (2005) Peroxiredoxins: a historical overview and speculative preview of novel mechanisms and emerging concepts in cell signaling. Free Radical Biol. Med. **38**, 1543–1552
7 Rhee, S. G., Kang, S. W., Jeong, W., Chang, T. S., Yang, K. S. and Woo, H. A. (2005) Intracellular messenger function of hydrogen peroxide and its regulation by peroxiredoxins. Curr. Opin. Cell Biol. **17**, 183–189
8 Toledano, M. B., Kumar, C., Le Moan, N., Spector, D. and Tacnet, F. (2007) The system biology of thiol redox system in *Escherichia coli* and yeast: differential functions in oxidative stress, iron metabolism and DNA synthesis. FEBS Lett. **581**, 3598–3607
9 Aslund, F., Berndt, K. D. and Holmgren, A. (1997) Redox potentials of glutaredoxins and other thiol-disulfide oxidoreductases of the thioredoxin superfamily determined by direct protein-protein redox equilibria. J. Biol. Chem. **272**, 30780–30786
10 Rouhier, N. and Jacquot, J. P. (2005) The plant multigenic family of thiol peroxidases. Free Radical Biol. Med. **38**, 1413–1421
11 Trotter, E. W. and Grant, C. M. (2003) Non-reciprocal regulation of the redox state of the glutathione-glutaredoxin and thioredoxin systems. EMBO Rep. **4**, 184–188
12 Schafer, F. Q. and Buettner, G. R. (2001) Redox environment of the cell as viewed through the redox state of the glutathione disulfide/glutathione couple. Free Radical Biol. Med. **30**, 1191–1212
13 Jones, D. P. (2006) Redefining oxidative stress. Antioxid. Redox Signal. **8**, 1865–1879
14 Kemp, M., Go, Y. M. and Jones, D. P. (2008) Nonequilibrium thermodynamics of thiol/disulfide redox systems: a perspective on redox systems biology. Free Radical Biol. Med. **44**, 921–937
15 Holmgren, A. (1979) Reduction of disulfides by thioredoxin. Exceptional reactivity of insulin and suggested functions of thioredoxin in mechanism of hormone action. J. Biol. Chem. **254**, 9113–9119
16 Peltoniemi, M. J., Karala, A. R., Jurvansuu, J. K., Kinnula, V. L. and Ruddock, L. W. (2006) Insights into deglutathionylation reactions. Different intermediates in the glutaredoxin and protein disulfide isomerase catalyzed reactions are defined by the gamma-linkage present in glutathione. J. Biol. Chem. **281**, 33107–33114
17 Akerman, S. E. and Muller, S. (2005) Peroxiredoxin-linked detoxification of hydroperoxides in *Toxoplasma gondii*. J. Biol. Chem. **280**, 564–570
18 Akerman, S. E. and Muller, S. (2003) 2-Cys peroxiredoxin PfTrx-Px1 is involved in the antioxidant defence of *Plasmodium falciparum*. Mol. Biochem. Parasitol. **130**, 75–81
19 Holmgren, A. (1979) Thioredoxin catalyzes the reduction of insulin disulfides by dithiothreitol and dihydrolipoamide. J. Biol. Chem. **254**, 9627–9632
20 Srinivasan, U., Mieyal, P. A. and Mieyal, J. J. (1997) pH profiles indicative of rate-limiting nucleophilic displacement in thioltransferase catalysis. Biochemistry **36**, 3199–3206
21 Ogusucu, R., Rettori, D., Munhoz, D. C., Netto, L. E. and Augusto, O. (2007) Reactions of yeast thioredoxin peroxidases I and II with hydrogen peroxide and peroxynitrite: rate constants by competitive kinetics. Free Radical Biol. Med. **42**, 326–334
22 Sayed, A. A. and Williams, D. L. (2004) Biochemical characterization of 2-Cys peroxiredoxins from *Schistosoma mansoni*. J. Biol. Chem. **279**, 26159–26166
23 Olivier, B. G., Rohwer, J. M. and Hofmeyr, J. H. (2005) Modelling cellular systems with PySCeS. Bioinformatics **21**, 560–561
24 Olivier, B. G. and Snoep, J. L. (2004) Web-based kinetic modelling using JWS Online. Bioinformatics **20**, 2143–2144
25 Fell, D. (1997) Understanding the Control of Metabolism, Portland Press, London
26 Reich, J. G. and Sel'kov, E. E. (1981) Energy Metabolism of the Cell, Academic Press, London
27 Nordstrand, K., Slund, F., Holmgren, A., Otting, G. and Berndt, K. D. (1999) NMR structure of *Escherichia coli* glutaredoxin 3-glutathione mixed disulfide complex: implications for the enzymatic mechanism. J. Mol. Biol. **286**, 541–552
28 Wynn, R., Cocco, M. J. and Richards, F. M. (1995) Mixed disulfide intermediates during the reduction of disulfides by *Escherichia coli* thioredoxin. Biochemistry **34**, 11807–11813
29 Wiita, A. P., Perez-Jimenez, R., Walther, K. A., Grater, F., Berne, B. J., Holmgren, A., Sanchez-Ruiz, J. M. and Fernandez, J. M. (2007) Probing the chemistry of thioredoxin catalysis with force. Nature **450**, 124–127
30 Wood, Z. A., Schroder, E., Robin Harris, J. and Poole, L. B. (2003) Structure, mechanism and regulation of peroxiredoxins. Trends Biochem. Sci. **28**, 32–40
31 Holmgren, A. (1984) Enzymatic reduction-oxidation of protein disulfides by thioredoxin. Methods Enzymol. **107**, 295–300
32 Vlamis-Gardikas, A., Aslund, F., Spyrou, G., Bergman, T. and Holmgren, A. (1997) Cloning, overexpression, and characterization of glutaredoxin 2, an atypical glutaredoxin from *Escherichia coli*. J. Biol. Chem. **272**, 11236–11243
33 Gallogly, M. M. and Mieyal, J. J. (2007) Mechanisms of reversible protein glutathionylation in redox signaling and oxidative stress. Curr. Opin. Pharmacol. **7**, 381–391
34 Holmgren, A., Johansson, C., Berndt, C., Lonn, M. E., Hudemann, C. and Lillig, C. H. (2005) Thiol redox control via thioredoxin and glutaredoxin systems. Biochem. Soc. Trans. **33**, 1375–1377
35 Mapson, L. W. and Isherwood, F. A. (1963) Glutathione reductase from germinated peas. Biochem. J. **86**, 173–191
36 Rohwer, J. M., Hanekom, A. J., Crous, C., Snoep, J. L. and Hofmeyr, J. H. (2006) Evaluation of a simplified generic bi-substrate rate equation for computational systems biology. Syst. Biol. **153**, 338–341
37 Holmgren, A. and Fagerstedt, M. (1982) The *in vivo* distribution of oxidized and reduced thioredoxin in *Escherichia coli*. J. Biol. Chem. **257**, 6926–6930
38 Munhoz, D. C. and Netto, L. E. (2004) Cytosolic thioredoxin peroxidase I and II are important defenses of yeast against organic hydroperoxide insult: catalases and peroxiredoxins cooperate in the decomposition of $H_2O_2$ by yeast. J. Biol. Chem. **279**, 35219–35227
39 Snoep, J. L., Bruggeman, F., Olivier, B. G. and Westerhoff, H. V. (2006) Towards building the silicon cell: a modular approach. BioSystems. **83**, 207–216
40 Powis, G. and Kirkpatrick, D. L. (2007) Thioredoxin signaling as a target for cancer therapy. Curr. Opin. Pharmacol. **7**, 392–397
41 Goldbeter, A. and Koshland, Jr, D. E. (1984) Ultrasensitivity in biochemical systems controlled by covalent modification. Interplay between zero-order and multistep effects. J. Biol. Chem. **259**, 14441–14447
42 Goldbeter, A. and Koshland, Jr, D. E. (1981) An amplified sensitivity arising from covalent modification in biological systems. Proc. Natl. Acad. Sci. U.S.A. **78**, 6840–6844
43 Kim, S. Y. and Ferrell, Jr, J. E. (2007) Substrate competition as a source of ultrasensitivity in the inactivation of Wee1. Cell **128**, 1133–1145


Received 28 May 2008/6 August 2008; accepted 12 August 2008
Published as BJ Immediate Publication 12 August 2008, doi:10.1042/BJ20080690

Biochem. J. (2009) **417**, 269–275 (Printed in Great Britain) doi:10.1042/BJ20080690

online data

## SUPPLEMENTARY ONLINE DATA

# Enzymes or redox couples? The kinetics of thioredoxin and glutaredoxin reactions in a systems biology context

Ché S. PILLAY, Jan-Hendrik S. HOFMEYR, Brett G. OLIVIER, Jacky L. SNOEP and Johann M. ROHWER[1]

Triple-J Group for Molecular Cell Physiology, Department of Biochemistry, Stellenbosch University, ZA-7602 Matieland, Stellenbosch, South Africa

### SUPPLEMENTARY DATA

The supplementary data provided here detail the values for parameters and variables used for the generic two-cycle model, and in the fitting of *in vitro* experimental datasets to the thioredoxin (Figure 2) and glutaredoxin (Figure 5A) models in the paper. The catalytic mechanism of thioredoxin reductase has been reported to proceed via a ternary complex mechanism [1,12], and glutathione reductase has been reported to proceed via a Ping Pong mechanism [3]. These mechanistic expressions were used in fitting experiments together with the Michaelis–Menten and generic [4] kinetic mechanisms respectively. In all cases, the reductase enzymes were modelled with irreversible kinetic expressions, as some of the parameters for their reversible expressions were not known. Details of the model of the thioredoxin/insulin assay from Figure 2 are summarized in Supplementary Table S1; the modelling results are given in Supplementary Table S2. The generic two-cycle model from Figure 3(B) is modelled in Supplementary Table S3. The parameters of the model of the deglutathionylation of a peptide substrate by Grx1 from Figure 5(A) are given in Supplementary Table S4; the modelling results are presented in Supplementary Table S5.

**Table S1 Parameters and values used for fitting the thioredoxin (Trx)/insulin assay dataset of Holmgren (Figure 2B in [5])**

| | Value | Reference |
|---|---|---|
| **Metabolites** | ($\mu$M) | |
| NADPH | 400 | [5] |
| NADP | 1 | [5] |
| Insulin (oxidized) | 30 | [5] |
| Insulin (reduced) | 1 | – |
| **Redoxin** | ($\mu$M) | |
| $Trx(SH)_2$ | 0.05 | [5] |
| Trx(SS) | 0.05 | [5] |
| **Thioredoxin reductase** | | |
| $k_{cat}$ | 1365 $min^{-1}$ | [6] |
| $K_{NADPH}$ | 1.2 $\mu$M | [3] |
| $K_{Trx(SS)}$ | 2.8 $\mu$M | [3] |
| [thioredoxin reductase] | 0.1 $\mu$M | [5] |

**Table S2 Fitted parameters and purported Michaelis–Menten parameters for the thioredoxin insulin model when the thioredoxin reductase reaction was assigned an irreversible ternary complex or a Michaelis–Menten kinetic mechanism**

| | Kinetic mechanism for thioredoxin reductase | |
|---|---|---|
| Fitted parameters | Ternary complex | Michaelis–Menten |
| $k_2$ | $3.83 \pm 0.29\,\mu M^{-1} \cdot min^{-1}$ | $3.82 \pm 0.29\,\mu M^{-1} \cdot min^{-1}$ |
| $K_{iNADPH}$ | $22.17 \pm 10.73\,\mu M$ | – |
| $r^2$ | 0.997 | 0.997 |
| **Purported Michaelis–Menten parameters for insulin reduction** | | |
| $K_m$ | 11. 53 $\mu$M | 12.12 $\mu$M |
| $V_{max}$ | 4.48 $\mu M \cdot min^{-1}$ | 4.70 $\mu M \cdot min^{-1}$ |

**Table S3 The apparent Michaelis–Menten parameters of a two-cycle redoxin system are sensitive to changes in the other parameters of the system**

Basic kinetic parameters of a two-cycle redoxin system were varied and the effect on the apparent Michaelis–Menten parameters for the reduction of *C* (Scheme 2) was determined. The parameters varied were: the limiting rate for a NADPH reductase ($V_{XR}$) in the system; $m_t$, the total concentration of the *M*/*M*′ redox couple; and $n_t$, the total concentration of the *N*/*N*′ couple (Scheme 2). *Goodness of fit to the Lineweaver–Burk plot.

| Model parameters | | | | | Apparent Michaelis–Menten parameters | | | | |
|---|---|---|---|---|---|---|---|---|---|
| $V_{XR}$ | $k_2$ | $m_t$ | $n_t$ | NADPH ($\mu$M) | $K_m$ | $V_{max}$ | $k_{cat}$ | $k_{cat}/K_m$ | $r^{2*}$ |
| 1 | 1 | 1 | 1 | 1 | 0.315 | 0.334 | 0.334 | 1.060 | 0.994 |
| 10 | 1 | 1 | 1 | 1 | 0.173 | 0.182 | 0.182 | 1.052 | 0.999 |
| 100 | 1 | 1 | 1 | 1 | 0.831 | 0.835 | 0.835 | 1.005 | 1.000 |
| 1 | 1 | 0.1 | 1 | 1 | 0.027 | 0.036 | 0.036 | 1.333 | 0.983 |
| 1 | 1 | 10 | 1 | 1 | 0.872 | 0.904 | 0.904 | 1.037 | 0.993 |
| 1 | 1 | 1 | 0.1 | 1 | 0.859 | 0.086 | 0.863 | 1.005 | 1.000 |
| 1 | 1 | 1 | 10 | 1 | 0.172 | 1.815 | 0.181 | 1.052 | 0.999 |
| 1 | 1 | 1 | 1 | 10 | 0.395 | 0.389 | 0.389 | 0.984 | 1.000 |
| 1 | 1 | 1 | 1 | 100 | 0.421 | 0.415 | 0.415 | 0.986 | 1.000 |

**Table S4 Parameters and values used for fitting the Grx1 substrate saturation dataset of Peltoniemi et al. (Figure 3B in [7])**

| | Value | Reference |
|---|---|---|
| **Metabolites** | ($\mu$M) | |
| NADPH | 50 | [7] |
| NADP | 1 | – |
| GSH | 998 | [7] |
| GSSG | 1 | – |
| PSSG | 1 | – |
| PSH | 1 | – |
| **Redoxin** | ($\mu$M) | |
| $Grx(SH)_2$ | 0.01 | [7] |
| Grx(SS) | 0.01 | [7] |
| **Glutathione reductase** | | |
| $k_{cat}$ | 500 $s^{-1}$ | [8] |
| $K_{GSSG}$ | 55 $\mu$M | [3] |
| $K_{NADPH}$ | 3.8 $\mu$M | [3] |
| [glutathione reductase] | 0.02 $\mu$M | [7] |

[1] To whom correspondence should be addressed (email jr@sun.ac.za).

**Table S5 Fitted parameters for the dataset of Peltoniemi et al. (Figure 3B in [7]) when the glutathione reductase reaction was assigned an irreversible Ping Pong or a generic kinetic mechanism**

| | Kinetic mechanism | |
|---|---|---|
| Parameter | Ping Pong | Generic |
| $k_2$ | $4.75 \pm 0.33 \times 10^{-6}\ \mu M^{-2} \cdot s^{-1}$ | $4.78 \pm 0.34 \times 10^{-6}\ \mu M^{-2} \cdot s^{-1}$ |
| $k_3$ | $0.64 \pm 0.048\ \mu M^{-1} \cdot s^{-1}$ | $0.64 \pm 0.049\ \mu M^{-1} \cdot s^{-1}$ |
| $r^2$ | 0.990 | 0.990 |

## REFERENCES


1 Lennon, B. W. and Williams, Jr, C. H. (1996) Enzyme-monitored turnover of *Escherichia coli* thioredoxin reductase: insights for catalysis. Biochemistry **35**, 4704–4712



Received 28 May 2008/6 August 2008; accepted 12 August 2008
Published as BJ Immediate Publication 12 August 2008, doi:10.1042/BJ20080690



2 Lennon, B. W. and Williams, Jr, C. H. (1995) Effect of pyridine nucleotide on the oxidative half-reaction of *Escherichia coli* thioredoxin reductase. Biochemistry **34**, 3670–3677
3 Williams, Jr, C. H. (1976) Flavin-Containing Dehydrogenases, Academic Press, New York
4 Rohwer, J. M., Hanekom, A. J., Crous, C., Snoep, J. L. and Hofmeyr, J. H. (2006) Evaluation of a simplified generic bi-substrate rate equation for computational systems biology. Syst. Biol. **153**, 338–341
5 Holmgren, A. (1979) Reduction of disulfides by thioredoxin: exceptional reactivity of insulin and suggested functions of thioredoxin in mechanism of hormone action. J. Biol. Chem. **254**, 9113–9119
6 Gleason, F. K., Lim, C. J., Gerami-Nejad, M. and Fuchs, J. A. (1990) Characterization of *Escherichia coli* thioredoxins with altered active site residues. Biochemistry **29**, 3701–3709
7 Peltoniemi, M. J., Karala, A. R., Jurvansuu, J. K., Kinnula, V. L. and Ruddock, L. W. (2006) Insights into deglutathionylation reactions: different intermediates in the glutaredoxin and protein disulfide isomerase catalyzed reactions are defined by the $\gamma$-linkage present in glutathione. J. Biol. Chem. **281**, 33107–33114
8 Massey, V. and Williams, Jr, C. H. (1965) On the reaction mechanism of yeast glutathione reductase. J. Biol. Chem. **240**, 4470–4480